Design of a bioinspired cownose ray robot

Giovanni Bianchi[a] and Simone Cinquemani[a]

[a]Politecnico di Milano, Dipartimento di Meccanica, Via La Masa 1, 20156, Milano, Italy

ABSTRACT

Fish swimming is a promising source of inspiration for novel and efficient propulsion mechanisms for autonomous underwater vehicles, as fishes swim with excellent energy efficiency and high maneuverability. Among the locomotion strategies of aquatic animals, the swimming mode of batoids is one of the most interesting, as these fishes swim with high energy efficiency, and they are capable of performing maneuvers with great agility. These advantages are mainly due to the fin geometry and the kinematics of their movement. The fish develops a traveling wave from the leading edge to the trailing edge of the fin, the amplitude of which increases towards the tip of the fin. This wave pushes the water backward, giving the fish a forward thrust due to momentum conservation. The motion of the fin of a cownose ray has been studied, and a biomimetic swimming robot inspired by the cownose ray has been designed and realized. Each fin is made of silicone sheets, and it is moved by three mechanisms whose kinematics replicate the fin deformation. Each mechanism is driven by an independent servomotor, creating a traveling wave on the fin whose frequency, wavelength, and amplitude can be modulated. The motors, battery, and electronics are housed in the central body of the robot, which is rigid. This paper describes the robot's design and construction.

Keywords: Bioinspiration, robot, fish, swimming, AUV, cownose ray, batoid, fin propulsion

1. INTRODUCTION

Fishes outperform conventional propellers in energy efficiency and maneuverability; therefore, they are source of inspiration for many autonomous underwater vehicles (AUVs), that find application in tasks requiring long endurance and great agility, such as environmental monitoring, surveillance, and search & rescue operations.[1]
The locomotion strategy adopted by batoid fishes is one of the most interesting since it meets all these characteristics. The Batoid order includes mantas and stingrays, which propel themselves by flapping their large pectoral fins. The motion of their fins is featured by a wave traveling from the fish's head to its tail, that pushes water backward, so that the fish gains thrust thanks to momentum conservation.[2,3] This type of locomotion is identified as oscillatory if less than a half-wave is present on the fin or undulatory otherwise. Oscillatory swimming is characteristic of migratory fishes that roam through the ocean at high speed, whereas undulatory swimming is distinctive of small species that need great maneuverability and live in narrow environments.[4]
Among batoids, the fish taken as a source of inspiration for developing a robot is the cownose ray (*Rhinoptera Bonasus*), a medium-sized fish, moving its fins in an oscillatory fashion. Thanks to their outstanding swimming performances, they have inspired the design of several underwater robots,[1] and some of them are briefly described in the following paragraph.

Several robots that take inspiration from a batoid fish use a single actuator for each fin, and the traveling wave is passively obtained thanks to the flexibility of the fin itself. An example is the robot developed by Chew et al.,[5] which features a rigid central body containing two servomotors that actuate the bionic fins, which are thin foils with a rigid leading-edge.
Other robots use a single mechanism to move the fin, but they actuate two degrees of freedom: the flapping motion and the twist angle of the fin, so that, properly combining these two motions, they can reproduce the oscillating movement of a fin of a batoid fish. An example of a robot of this kind is the one realized by Chen

Further author information: (Send correspondence to Giovanni Bianchi)
Giovanni Bianchi: E-mail: giovanni.bianchi@polimi.it, Telephone: (+39) 02 23998265
Simone Cinquemani: E-mail: simone.cinquemani@polimi.it

et al.,[6] featured by fins composed of a flexible elastomer and actuated by an electroactive polymer beam, which performs both flapping and twisting motions. Another robot belonging to this category is the Aqua Ray robot, made by Festo,[7] which is actuated by hydraulic bionic fin muscles, and three antagonistic muscles give the robot the ability to flap and twist its fins to recreate an oscillatory motion.
Finally, other robots actuate their fins with several independent mechanisms. These robots are characterized by extraordinary maneuverability because the independent actuation of different mechanisms gives the possibility to modulate the wave propagation. For example, the MantaBot[8] has fins composed of cable-driven tensegrity structures surrounded by a flexible elastomer. The bionic fish developed by Cai et al.[9] accurately reproduces the traveling wave present on a cownose ray, and it is characterized by high maneuverability thanks to its flexible fins actuated by several motors.

The robot object of this work has deformable fins actuated by three independent mechanisms. Therefore, it is possible to achieve excellent maneuverability by adjusting the parameters of the fin kinematics, such as the oscillation frequency and the phase shift between the mechanisms. In this paper, the robot design and construction are presented.

2. DESIGN OF THE FINS

The overall dimensions of the robot replicate the dimensions of the real cownose ray, so the length of the robot is about 0.58m, and its width from fin tip to fin tip corresponds to about 1 m. In addition, the robot is supposed to be neutrally buoyant, so its mass is tuned to reach the corresponding mass of the water volume displaced.

The first step is the study of fin geometry and fin motion; then, kinematic synthesis of a mechanism approximating the fin movement is carried out. The fin contour is taken from the literature,[10] and it is obtained by reconstructing a curve that follows the profile of a cownose ray fin. The cross sections along the span of a fin are approximated with a series of aerodynamic profiles with gradient changes from a large profile in the body center to a thin profile at the fin tip.[9] The robot's external surface and dimensions are shown in Figure 1.

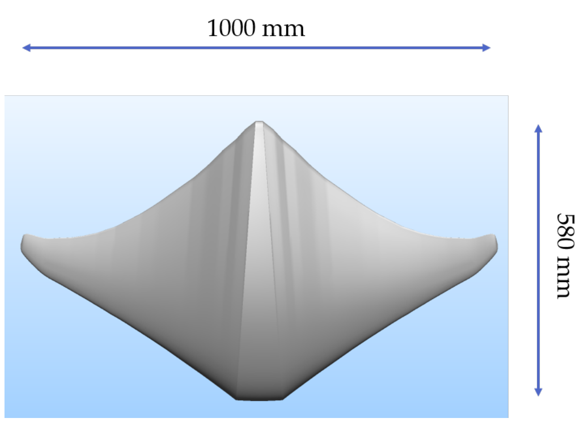

(a) Dimensions of the external surface of the robot

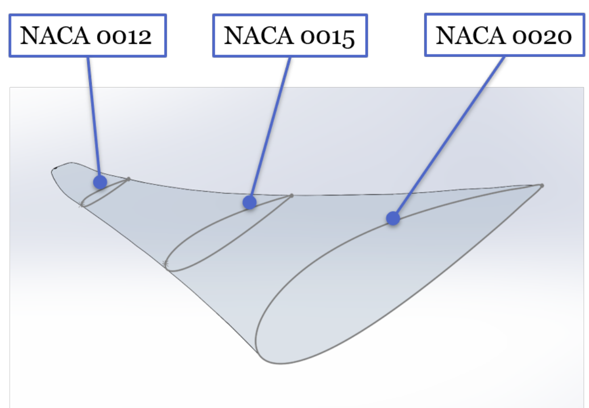

(b) Cross sections of a fin

Figure 1: Shape and dimension of the cownose ray robot

The fins' mechanisms were designed to mimic the fin deformation responsible for thrust generation accurately. The motion of the fin consists of a wave traveling from the head to the tail with amplitude increasing towards the fin tip. Since the wavelength is more than double the chord length of the fish, three mechanisms are enough to reproduce the traveling wave, and they are positioned near the head, in the center, and near the tail.[10] The equations describing the fin deformation can be obtained from Russo et al.,[11] who analyzed the skeletal structure of a cownose ray and related it to the fin kinematics. Assuming that the deformation is continuous along the fin, the deformation of every fin section can be represented by the following equations:

$$\begin{cases} y(s,t) = \dfrac{1-\cos\left[\theta_{max} s \sin\left(\phi x - \omega t\right)\right]}{\theta_{max}\sin\left(\phi x - \omega t\right)} \\ z(s,t) = \dfrac{\sin\left[\theta_{max} s \sin\left(\phi x - \omega t\right)\right]}{\theta_{max}\sin\left(\phi x - \omega t\right)} \end{cases} \tag{1}$$

where y and z are depicted in 2, ω is the frequency of fin flapping, ϕ is the wave number along the fin, θ_{max} is the angle formed by the fin at its tip and s is the curvilinear abscissa along the fin span.

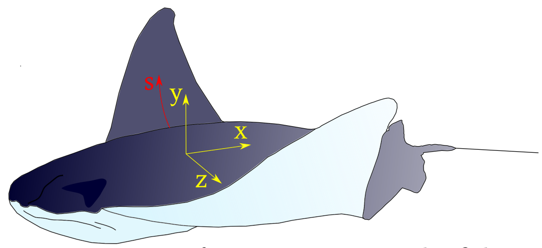

Figure 2: Reference system on the fish

The mechanisms in the front and in the rear are exactly the same, and they are shown in Figure 3.

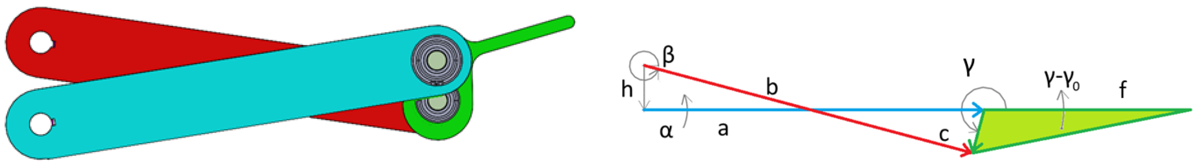

(a) CAD model (b) Kinematic diagram

Figure 3: Frontal and rear mechanism of the pectoral fins

The mechanism is a crossed four-bar linkage where the light-blue link is connected to the motor. The link lengths have been optimized to reproduce at best the deformation of the corresponding fin section with the minimum area error method described by Cai et al.,[12] which consists in finding the optimal combination of link lengths that minimizes the area between the real deformed curve and the shape obtained with the three links. The optimization procedure is performed considering a dimensionless problem and considering the overall length of the fin span in the central section.

Hence, the first step is to solve the kinematics of the mechanism to calculate the area below it. Since the motor is connected to the link a, shown in light-blue, the angle α corresponds to the rotation of the motor and it is convenient to express all other variables as functions of α. By projecting on the x and y axes, the following expression is obtained:

$$\begin{cases} b\cos\beta = a\cos\alpha + c\cos\gamma \\ h + b\sin\beta = a\sin\alpha + c\sin\gamma \end{cases} \tag{2}$$

Rearranging the terms, Equation 2 becomes:

$$\begin{cases} c\cos\gamma = -a\cos\alpha + b\cos\beta \\ c\sin\gamma = -a\sin\alpha + h + b\sin\beta \end{cases} \tag{3}$$

Squaring both equations and summing them together, it is possible to obtain an equation with the only variable β, which, after some simplifications, is equal to:

$$c^2 = a^2 + b^2 + h^2 - 2h\,(a \sin\alpha - b \sin\beta) - 2ab\cos(\alpha - \beta) \tag{4}$$

Then, it is possible to find the angles β and γ.

$$\beta = 2\arctan\left(\frac{\sqrt{2a^2c^2 - b^4 - c^4 + 6a^2b^2 - a^4 + 2b^2c^2 - 2a^2h^2(1 - 2\sin^2\alpha) + 2b^2h^2 + 2c^2h^2 + 4ah\sin\alpha(-h^2 - a^2 + b^2 + c^2)} + 2bh + 2ab\sin\alpha}{a^2 + 2ab\cos\alpha + 2ah\sin\alpha + b^2 - c^2 + h^2}\right) \tag{5}$$

$$\gamma = \arccos\left(\frac{b\cos\beta - a\cos\alpha}{c}\right) \tag{6}$$

Another critical aspect of the kinematics of the frontal and rear mechanism is that the c link, shown in green, must be in a horizontal position when the angle α is equal to zero. According to Figure 3, when α is 0, also $\gamma - \gamma_0$ must be equal to zero. Hence, it is necessary to find the correct value of γ_0 to satisfy this condition, which for this configuration is equal to $-105.07°$.

The central mechanism of the fin, shown in Figure 4, is featured by the same kinematic diagram repeated twice; thus, the kinematics can be solved using the same set of equations, and the angle δ_0, which allows the final link to be in a horizontal position when $\alpha = 0$ is $-105.07°$.

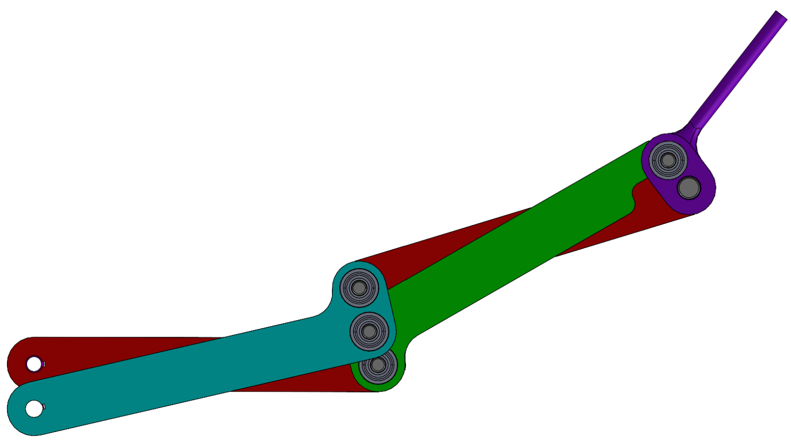

(a) CAD model

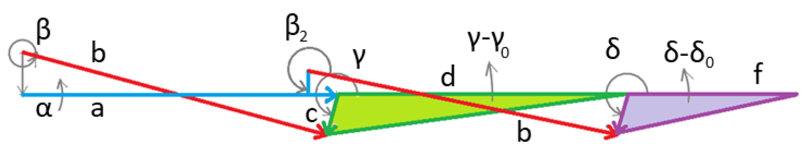

(b) Kinematic diagram

Figure 4: Central mechanism of the pectoral fins

After having solved the kinematics of the mechanisms, it is possible to calculate the area below the links, which is:

$$\begin{aligned}\tilde{A} = & \frac{a^2 \sin\alpha\cos\alpha}{2} + \frac{(2a\sin\alpha + c\sin(\gamma - \gamma_0))\,c\cos(\gamma - \gamma_0)}{2} \\ & + \frac{(2a\sin\alpha + 2c\sin(\gamma - \gamma_0) + d\sin(\delta - \delta_0))\,d\cos(\delta - \delta_0)}{2}\end{aligned} \tag{7}$$

The angle α is a sinusoidal function of time, and the variable θ can be introduced as a cyclical variable. The amplitude of the oscillation of α is unknown and it is determined together with the other parameters of the optimization:

$$\alpha = X \sin(\phi x - \omega t) = X \sin\theta. \tag{8}$$

The area below the real curve is obtained by integrating Equation 1 along z, and it results:

$$A = \frac{z_{max}}{\theta_{max}\sin(\phi x - \omega t)} \mp \frac{1}{2}\left(z_{max}\sqrt{\frac{1}{(\theta_{max}\sin(\phi x - \omega t))^2} - z_{max}^2} \pm \frac{\arcsin(z_{max}\theta_{max}\sin(\phi x - \omega t))}{(\theta_{max}\sin(\phi x - \omega t))^2}\right). \tag{9}$$

Considering that the sum of the length of the three links must be equal to the length of the span of the fin, it is possible to write:

$$f = 1 - a - d. \tag{10}$$

Therefore, the area below the links $\tilde{A}$ of Equation 7 is a function of five variables: a, b, c, d, h, X. The function to minimize is the difference between the two areas for all the time instants of a period of fin oscillation, i.e., for all the angles θ from 0 to 2π, and it is written as:

$$S = \sum_{\theta=0}^{2\pi} |A(\theta) - \tilde{A}(\theta)|. \tag{11}$$

The result of the link lengths optimization is shown in Figure 5, and the resulting link lengths are listed in Table 1.

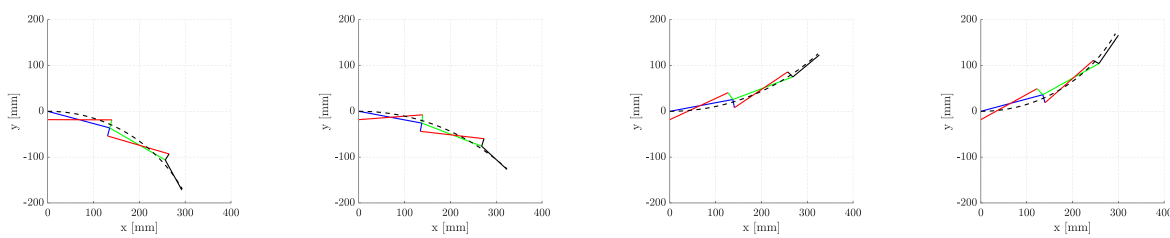

(a) (b) (c) (d)

Figure 5: Result of the optimization of link lengths

Table 1: Link lengths resulting from optimization

a	140 mm
b	140 mm
c	18.2 mm
d	140 mm
f	70.5 mm
h	18.2 mm

When the mechanisms move with a great phase shift, the distance between corresponding points of different mechanisms increases, requiring that the external surface is stretchable enough to allow such a large deformation.

Although the material of the fins is highly flexible and able to bear such an elongation, this is still not desirable, as the elastic force would be an additional load for the motors reducing the torque available to move the surrounding water. Therefore, to limit this problem, the last link, c, shown in green, in the front and rear mechanisms, is connected by means of spherical bearings to a and b links so that an out-of-plane rotation is allowed and the tip of the front and the rear mechanisms can bend toward the center when a great phase shift makes the distance increase. Conversely, all the bearings of the central mechanisms are cylindrical.

The fins are the most crucial part of the robot because they generate thrust with their movement and deformation. Therefore, it is fundamental to design fins that follow the movement imposed by the mechanisms generating a traveling wave without creating folds and losing hydrodynamic efficiency so that all the advantages of this locomotion principle are exploited. Another essential requirement of the fins is their impermeability because they constitute the external surface of the robot, and they waterproof the internal part.

The robot skin is made of silicone rubber sheets. This material is immensely elastic, allowing a maximum elongation of 600% before breaking, having a Young modulus between 0.2 and 4MPa. Using sheets 0.2mm thick, it is possible to attach them to the central body and the mechanisms keeping them stretched so that they are never loose and never create folds, but, thanks to the material elasticity, they do not generate undesired stresses on the mechanisms.
To always keep the sheets in the correct position, a flexible structure is created along the fin edges, represented in Figure 6, showing the complete assembly of the robot with fins made of silicone sheets.

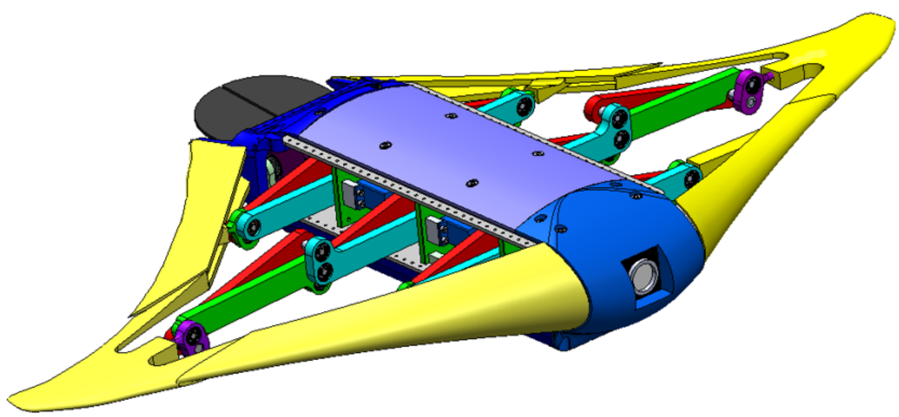

Figure 6: Robot with the support structure for the fins made of silicone sheet

Not to deplete the elastic properties of the fins, this structure must allow a high deformation, so it is made of TPU, which is a material suitable for 3D printing with mechanical characteristics similar to rubber. Furthermore, the Young modulus of TPU is about 40MPa; thus, this structure would significantly increase the stiffness of the fin, especially against tension, while leaving its bending stiffness almost unchanged. However, this problem can be solved by designing a constraint that allows some relative motion between this structure and the mechanisms. The structure and the silicone rubber sheets are glued to the central part of the robot, whereas the constraint between the structure and the mechanisms is a mechanical coupling. The last link of each mechanism is inserted in a pocket of the same shape present in the TPU structure, leaving a few centimeters of axial clearance so that, when there is a significant phase shift between mechanisms, the structure needs to elongate of a small quantity. Moreover, the last link of the central mechanism has a circular cross-section so that the structure is also free to rotate around it to avoid stresses when the phase shift between mechanisms is significant, and the front and the rear mechanisms move in opposite directions.

The tail of the robot acts as a rudder, and it has the function of correcting the pitch rotation during forward swimming and of improving the robot's maneuverability during floating and diving maneuvers. The tail is composed of two rudders so that they can be moved independently and help stability during turning maneuvers, and the motors moving the tail are the same as those moving the mechanisms of the pectoral fins. The links and the frames are made of aluminum, and some plastic 3D-printed parts are placed on the top, in the front, and in the back to have a hydrodynamic profile. In the front, a pocket to hold a video camera is present.

The robot has been assembled, as shown in Figure 7, where some construction phases are presented, highlighting the mechanisms, the structure of the fin and the final assembly of the robot.

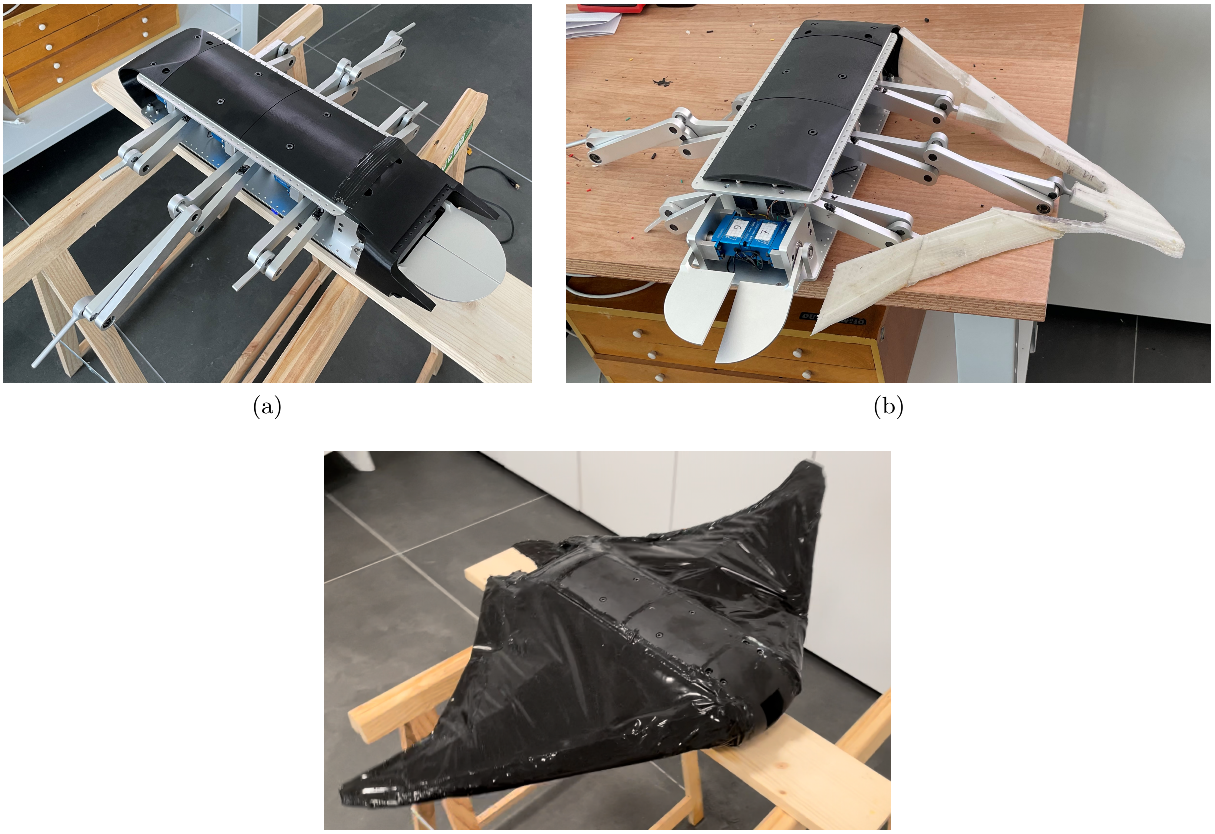

(a) (b) (c)

Figure 7: Bioinspired robot

To make the robot neutrally buoyant some ballasts have been attached below the rigid part in the body center. The mass of the robot with ballasts is 11kg.

3. ROBOT COMPONENTS

The electronic board of the robot is Arduino Due, which is featured by high computational power and a large number of input and output pins while remaining economical and simple to program. The electronic circuit of the robot includes:

- **8 servomotors**: three motors move each pectoral fin, and two are employed to move the tail. The selected motors are brushless servomotors *PowerHD 40 waterproof*. They are IP68 certified and provide a torque of 3.92Nm when powered at 8V.
- **6 encoders**: they measure the angular position of the fin mechanisms since it is fundamental to have reliable feedback in order to synchronize fin mechanisms and give them the correct phase shift. The selected encoders are the AS5600 magnetic encoders.
- **Inertial Measurement Unit (IMU)**: it is composed of a 3-axes accelerometer and a 3-axes gyroscope needed to control the robot position and orientation while swimming.

- **Bluetooth module**: it is used to communicate wirelessly with the operator without removing sealing when the robot is outside of water.
- **SD card module**: it is needed to store navigation data since it is impossible to communicate wireless underwater.
- **Battery**: the chosen battery is a LiPo battery with 2 cells with a capacity of 5200 mAh and a rated voltage of 7.4V.

4. CONCLUSION

In this work, a bioinspired swimming robot has been designed and built. This robot replicates the locomotion strategy of the cownose ray, which is featured by high energy efficiency and maneuverability. In order to obtain the same swimming performances, the robot's fins have been optimized to reproduce at best the movement of the fins of its natural counterpart. The kinematic synthesis of the mechanisms actuating the fins has been carried out using an optimization method that allowed obtaining a good superimposition of the mechanisms and the correspondent cross-section of the fin. Furthermore, the silicone rubber sheets constituting the external surface of the fins are characterized by extremely high elasticity so that they deform following the desired fin movement without creating any folds. This allows keeping the fin surface smooth and maintaining high hydrodynamic efficiency. Mass and dimensions of the robot are similar to a real cownose ray, and the robot's mass distribution has been balanced thanks to the addition of some ballasts to make it neutrally buoyant. The robot has been built, and as future work, the control algorithm will be designed to perform underwater experiments, which will be useful to investigate the advantages of the batoid fish locomotion strategy.

REFERENCES

[1] Salazar, R., Fuentes, V., and Abdelkefi, A., "Classification of biological and bioinspired aquatic systems: A review," *Ocean Engineering* **148**, 75–114 (2018).

[2] Lighthill, M., "Hydromechanics of aquatic animal propulsion," *Annual Reviews on Fluid Mechanics* **1**, 413–446 (1969).

[3] Wu, T., "Hydromechanics of swimming of fishes and cetaceans," *Advances in Applied Mechanics* **11**, 1–63 (1971).

[4] Rosemberger, L., "Pectoral fin locomotion in batoid fishes: undulation versus oscillation," *Journal of Experimental Biology* **204**, 379–394 (2001).

[5] Chew, C., Lim, Q., and Yeo, K., "Development of propulsion mechanism for robot manta ray," in [*Proceedings of the 2015 IEEE Conference on Robotics and Biomimetics*], (2015).

[6] Chen, Z., Um, T., Zhu, J., and Bart-Smith, H., "Bio-inspired robotic cownose ray propelled by electroactive polymer pectoral fin," in [*Proceedings of the ASME 2011 International Mechanical Engineering Congress & Exposition*], (2011).

[7] Festo, "Aqua ray," tech. rep. (2007).

[8] Fish, F. E., Schreiber, C. M., Moored, K. W., Liu, G., Dong, H., and Bart-Smith, H., "Hydrodynamic performance of aquatic flapping: Efficiency of underwater flight in the manta," *Aerospace* **3**(20), 3030020 (2016).

[9] Cai, Y., Bi, S., Li, G., Hildre, H., and Zhang, H., "From natural complexity to biomimetic simplification: Realization of bionic fish inspired by the cownose ray," *IEEE Robotics and automation magazine* **99**, 1–13 (2018).

[10] Cai, Y., Bi, S., and Zhang, L., "Design and implication of a bionic pectoral fin imitating cow-nosed ray," in [*The 2010 IEEE/RSJ International Conference on Intelligent Robots and Systems*], (2010).

[11] Russo, R., Blemker, S., Fish, F., and Bart-Smith, H., "Biomechanical model of batoid (skates and rays) pectoral fins predicts the influence of skeletal structure on fin kinematics: implications for bio-inspired design," *Bioinspiration & Biomimetics* **10**, 046002 (2015).

[12] Cai, Y., Bi, S., and Zheng, L., "Design optimization of a bionic fish with multi-joint fin rays," *Advanced Robotics* **26**, 177–196 (2012).